Transmission of LG beams in 128×40 Gbps MDM-PDM employed High Capacity Free Space System under severe climate conditions

VIVEK ARYA*
Department of ECE, UIE, Chandigarh University, Mohali-140413, Punjab, India

An integrated polarization division multiplexing and mode division multiplexing based free space optics system using Laguerre-Gaussian (LG) is designed. It is investigated for four LG modes with 128 users under different weather scenarios. It is realized that maximum 4100 m range can be obtained under very clear condition at 128×40 Gbps data rate. Also, the system can sustain beam divergence of 5.3 mrad at 2.56 Tbps throughput over 2000 m range. Besides, the system offers quality factor of >6, with -6 dBm received optical power for all modes and shows its superiority than existing designs under very clear, clear, light and moderate rain conditions.

(Received January 8, 2025; accepted August 4, 2025)

Keywords: 5G, FSO, LG, MDM

1. Introduction

The requirement for high transmission rate, ultra-reliability, low latency, massive connectivity, as well as raised device density is improving exponentially owing to several services like virtual/augmented reality, internet of things (IoT), intelligent infrastructures, and real-time e-healthcare, etc. [1]. Fulfilling ubiquitous global coverage forms future communication via universal & seamless connectivity [2]. Next generation optical networks require an appropriate infrastructure to offer high-speed transmission, flexible bandwidth, less latency, low cost, and reconfigurable edge node design. Because of severe multimedia services growth viz. video on demand, 4K/8K video streaming, broadband Internet, high-definition TV, video conferencing, 6G mobile communications, and voice over IP, the wireless network suffer the over data traffic crowdedness [3].

Free space optics (FSO), a license free optical wireless technology has received much interest numerous applications. It is a significant solution for last mile link problems, especially for future communication networks. FSO can be easily employed when the fiber installation is costly or not feasible. It guarantee a line-of-sight (LoS) high data rate wireless communication over long-reach (~1000 km) and it is a promising technology to scale down ultra-high bandwidth challenges in beyond 5G networks [4].

Further, polarization Division Multiplexing (PDM) is considered as an effective technology for enhancing system throughput as well as spectrum efficiency by employing dual orthogonal polarizations of each carrier to attain double the system throughput. Again, the usage of a multi-carrier transmission scheme could too enhance transmission range where various subcarriers are modulated in orthogonal and parallel, causing the evasion of inter-symbol Interference [5].

Furthermore, mode division multiplexing (MDM) is an emerging technique incorporating Eigen modes is utilized to transmit synchronously independent data streams over different spatial modes. These modes enhance the link capacity and used for the propagation of a several channels on distinct generated modes. Moreover, MDM can further enhance spectral bandwidth of the link by integrating it with PDM where PDM utilizes dual polarization [6]. In MDM, the realization of Laguerre-Gaussian (LG) faces issues depending on various factors strongly concerned with FSO media such as scattering, absorption and turbulence-induced fading [4].

Recently, in [5], an 8 channel MDM-PDM system using orthogonal frequency division multiplexing (OFDM) scheme over 48000 km inter-satellite link at 5.12Tbps data rate is presented. In [2], a radio over fiber (RoF) system using 64 channel dense wavelength division multiplexing (DWDM) scheme based differential quadrature phase-shift keying (DQPSK) over 1600 km at 1.792 Tbps data rate is realized. In [6], an 80 Gbps PDM based orbital angular momentum (OAM) system using offset-quadrature-phase shift keying (OQPSK) at 6km FSO range under clear air is realized. In [7], an OAM based wavelength division multiplexing (WDM) FSO system using pulse amplitude modulation level-4 over 162 m range at 1600 Gbps data rate is investigated under weak-to-strong turbulence. In another work, a WDM-FSO system over 600 m range at 160 Gbps transmission rate is presented for the 5G communication systems [8]. In [9], an OAM based PON system incorporating 0.4 m FSO link at 10 bps data rate is explored for future ultrahigh-capacity optical networks. Also, in [10], an underwater optical communication system incorporating attenuation loss of 49.34 dB/m over 1600 m range at 200 Gbps data rate is presented.

Again, in the last few years, several significant optical systems have been advanced, where the major objectives are to enhance the data rate, transmission reliability, spectral efficiency and channel capacity [20-21]. LG based PDM/MDM-FSO system is employed in this work where LG beams are used to encode information on polarized laser beam for transmitting over FSO link. It is suitable for next-generation FSO systems. Also, it offers benefits for next generation technologies like quantum technologies, satellite communication etc. due to very low power consumption as well as ease of mode generation [22-23].

In Section 2, the proposed design of PDM/MDM-FSO system using LG beams under severe climate conditions are investigated. Section 3 explains the obtained results with discussions followed by conclusion along with future scope in Section 4.

2. Proposed system

The schematic diagram of the proposed MDM/PDM-FSO system using LG beams is exhibited in Fig. 1.

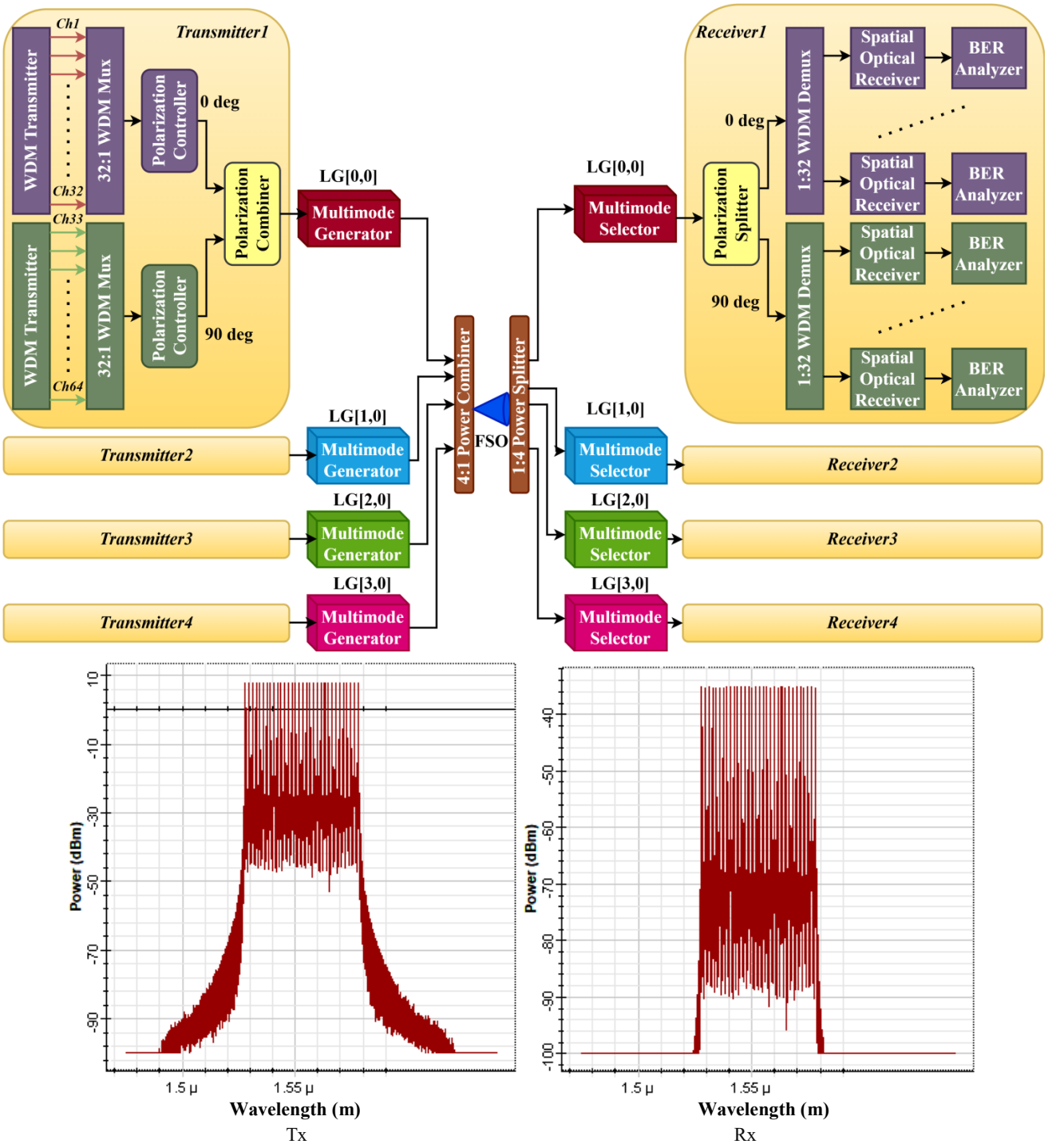

Fig. 1. Setup for proposed PDM/MDM-FSO system; insets: optical spectra at transmitter and receiver (colour online)

Only a single transmitter as well as receiver is shown out of four transceivers for simplification as well as better understanding. At transmitter, a 32:1 WDM transmitter array's (190-196.2 THz) lasers power is forwarded to a 32:1 WDM multiplexer for realizing Tx1 to Tx32 where each Tx incorporates 10 dBm input power at 40 Gbps data rate. Likewise, other Tx33 to Tx64 data is obtained to realize the PDM technique. Two orthogonal polarization controllers are employed for each 32 channel WDM transmitter. A multimode generator is used to generate different LG beams viz. LG[0,0], LG[1,0], LG[2,0] and LG[3,0] as depicted in Fig. 2. After this, the data received from total 128 channels operating at different MDM modes is combined by a 4:1 power combiner to pass over a FSO link under the impact of diverse climate conditions.

At receiver, a 1:4 power splitter is used to split different beams to specific mode selector followed by a dual orthogonal polarization splitter. In each receiver section, a 1:32 WDM de-multiplexer transfers the signals to different spatial optical receivers having PIN photodiode and low pass filter for obtaining electrical data with minor noise. For evaluating the system performance, BER, Q-factor and eye patterns are observed by a BER analyzer. The main parameters of the proposed model are tabulated in Table 1 [11-13]. Table 2 depicts various channels' frequencies used in the system.

Table 1.Simulation parameters [14]-[16].

Parameters		**Value**
Frequency		190-196.2 THz
Throughput		40 Gbps
No. of channels		128
Input power		10 dBm
MDM mode		LG[0,0],LG[1,0], LG[2,0], LG[3,0]
FSO range		3500-4100 m
FSO attenuation	Very clear	0.15 dB/km
	Clear	0.299 dB/km
	Light Rain (12 mm/hr precipitation)	0.62 dB/km
	Moderate rain	2.62 dB/km
Additional, Tx and Rx losses		0.1 dB
Weak turbulence		10^{-17} $m^{-2/3}$
Geometrical loss		Yes
Tx/Rx aperture diameter		10 cm
Tx/Rx loss		0.1dB
Shot noise		Yes
Beam divergence		3-6 mrad
Responsitivity		0.9A/W
Dark current		10 nA

Table 2. Channel frequencies used in the system

Channel	**Frequency (THz)**
channel_1	190
channel_2	190.2
channel_3	190.4
channel_4	190.6
channel_5	190.8
channel_6	191
channel_7	191.2
channel_8	191.4
channel_9	191.6
channel_10	191.8
channel_11	192
channel_12	192.2
channel_13	192.4
channel_14	192.6
channel_15	192.8
channel_16	193
channel_17	193.2
channel_18	193.4
channel_19	193.6
channel_20	193.8
channel_21	194
channel_22	194.2
channel_23	194.4
channel_24	194.6
channel_25	194.8
channel_26	195
channel_27	195.2
channel_28	195.4
channel_29	195.6
channel_30	195.8
channel_31	196
channel_32	196.2
channel_33	190
channel_64	196.2

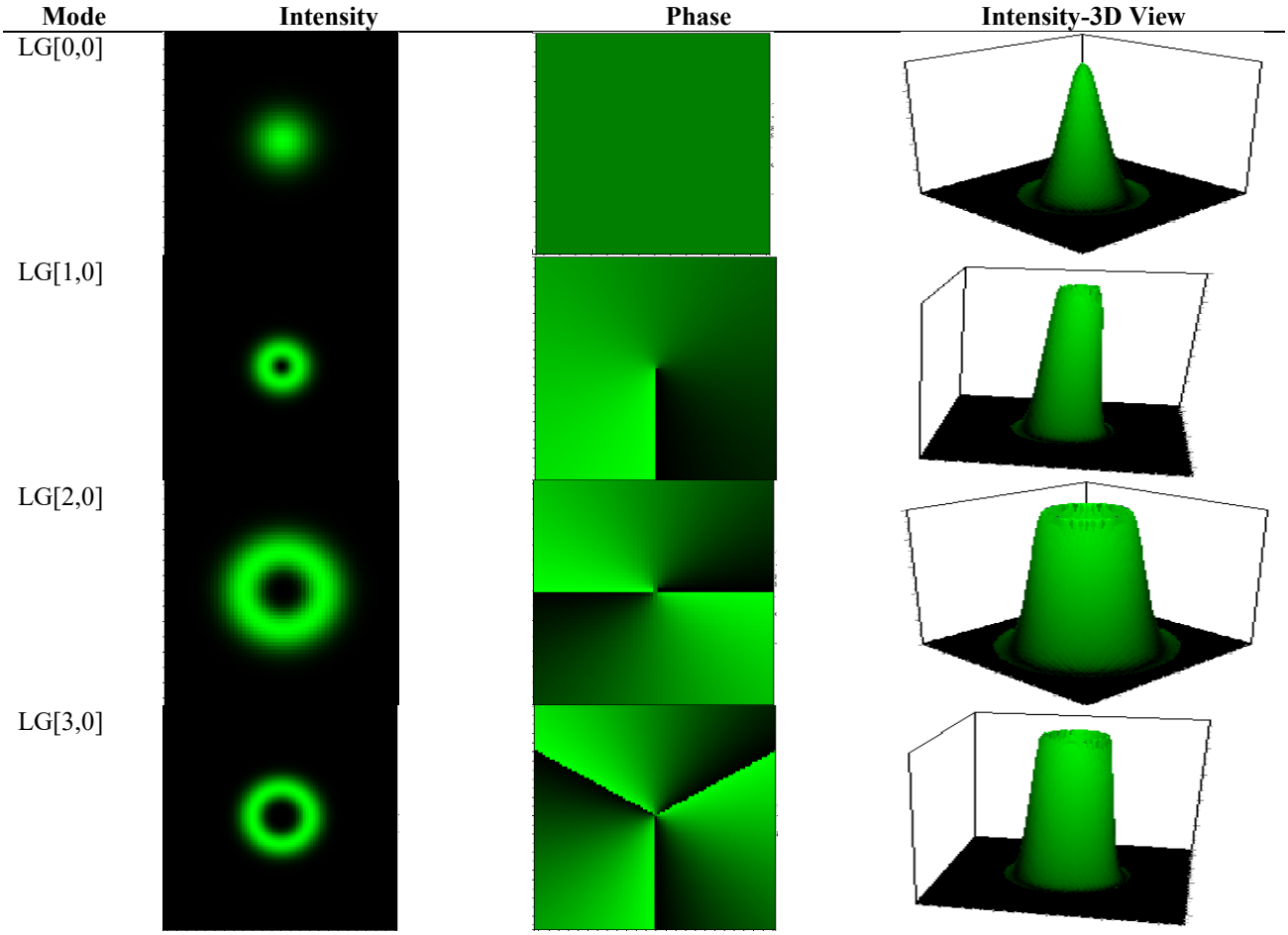

Fig. 2. Generated LG modes (colour online)

Mathematically, the generated LG modes are represented as [17], [18]:

$$\Phi_{s,l}(r,\emptyset) = \left(\frac{2r^2}{\omega_0^2}\right)^{\left|\frac{l}{2}\right|} . L_s^l\left(\frac{2r^2}{\omega_0^2}\right) . exp\left(\frac{r^2}{\omega_0^2}\right) . exp\left(\mathrm{j}\frac{\pi r^2}{\lambda R_0}\right) \begin{cases} cos(l\emptyset), n \geq 0 \\ \sin(l\emptyset), n \geq 0 \end{cases} \quad (1)$$

where R_0 means curvature radius, s & l mean azimuthal indices and radial indices, respectively, ω_0 means spot size, L_s & L_l are Laguerre polynomials.

3. Results and discussion

The proposed work is investigated in OptiSystem v.20 and its performance is measured under very clear, light rain and haze conditions considering Gamma-Gamma channel turbulence model as [16-18]:

$$f_g(g) = \frac{2(xy)^{\left(\frac{x+y}{2}\right)}}{\Gamma(x)\Gamma(y)} . g^{\left(\frac{x+y}{2}\right)-1} K_{x-y}\left[2(xyg)^{\frac{1}{2}}\right] \quad (2)$$

where $\Gamma(.)$ depicts Gamma function, K_{x-y} depicts modified Bessel function having large (y) & small (x) scale effective eddies of order $(x-y)$ and defined as [12]:

$$x = \frac{1}{\left[exp\left\{\frac{0.49k_0^2}{\left(1+0.18d^2+0.56k_0^{\frac{12}{5}}\right)^{\frac{7}{6}}}\right\}-1\right]} \quad (3)$$

and

$$y = \frac{1}{\left[exp\left\{\frac{0.51k_0^2\left(1+0.18d^2+0.56k_0^{\frac{12}{5}}\right)^{\frac{-5}{6}}}{\left(1+0.90d^2+0.62d^2k_0^{\frac{12}{5}}\right)^{\frac{5}{6}}}\right\}-1\right]} \quad (4)$$

where d depicts the spherical wave diameter, k_0^2 depicts Rytov variance. The attenuation due to rain is given as [17-19]:

$$R_{rain} = \beta R^t \quad (5)$$

where R is rain rate, β and $t$are coefficients depending on wavelength as well as temperature.

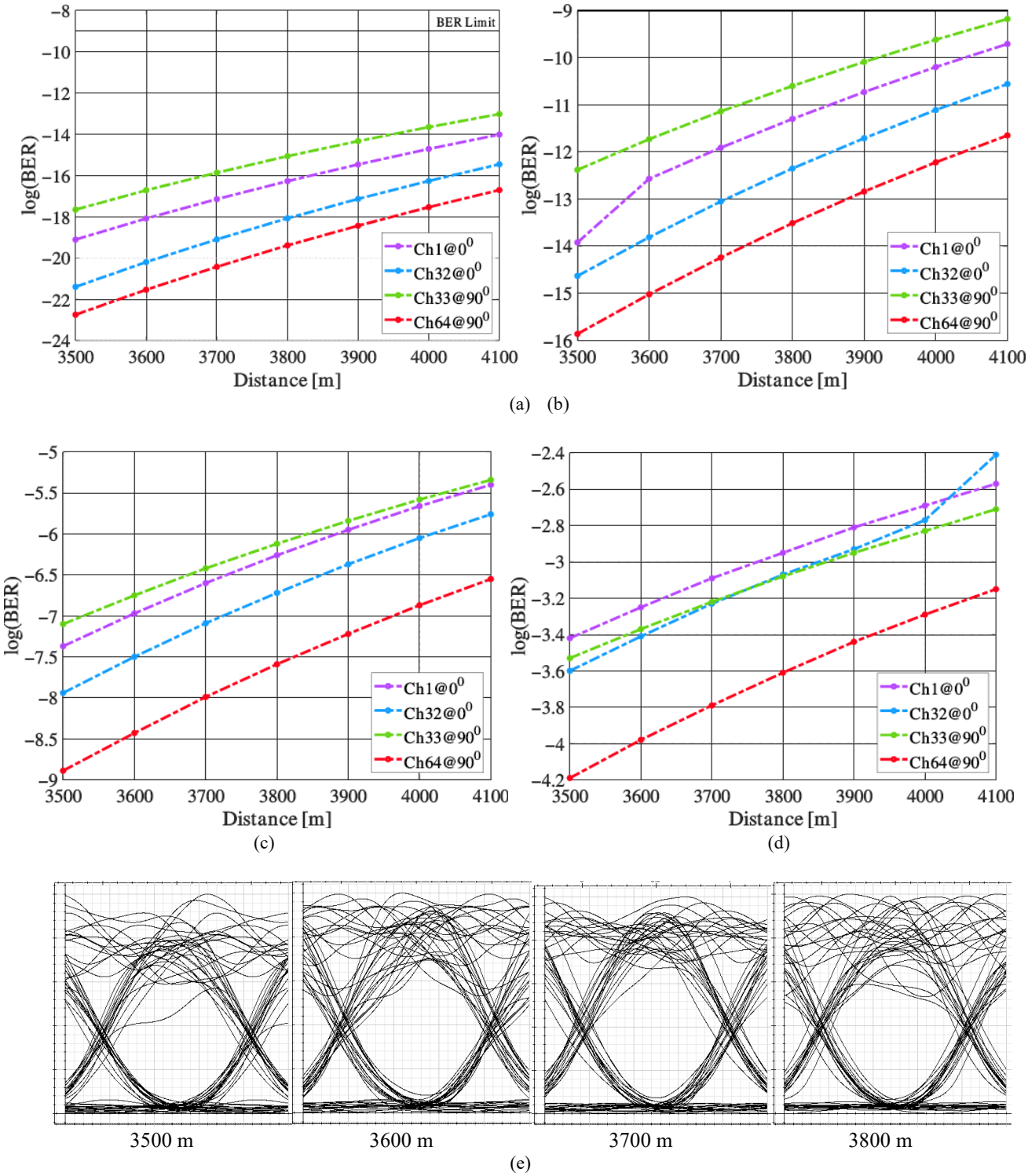

Fig. 3. Distance vs. BER for (a) LG[0,0], (b) LG[1,0], (c) LG[2,0], (d) LG[3,0], (e) eye patterns for LG[0,0] mode (colour online)

Fig. 3(a)-3(d) depicts the system BER performance for varied FSO distance under very clear condition for LG [0,0], LG[1,0], LG[2,0] and LG[3,0] modes respectively, at 0 and 90 deg angles. The system performs better for LG [0,0] followed by LG [1,0], LG [2,0] and LG [3,0] modes for orthogonal polarizations at BER limit of 10e-9. However, channel_64 at 90 deg performs best out of all channels viz. channel_32 at 0 deg, channel_1 at 0 deg and channel_33 at 90 deg considerably.

Fig. 3(a) and 3(b) exhibit maximum distance of 4100 m for all channels operating at different polarization angels under very clear condition at both LG[0,0] as well as LG[1,0] modes. Also, for LG[2,0] mode operating under very clear condition offers maximum 3500 m range for channel_64 at 90 deg while, < 3500 m for other channels, as depicted in Fig. 3(c). Moreover, 3(d) exhibits maximum FSO range of < 3500 m for all channels means their BER performance is less than that under very clear condition for LG[3,0], as depicted in Fig. 3(d). Moreover, 3(e) depict the clearly wide opened eye patterns depict the system optimum performance for LG[0,0] mode under very clear at varied ranges.

Out of all modes LG[0,0] mode offers minimal beam bivergence, less affected by free space turbulence, and incorporates higher coupling efficiency at receiver, thus outperforms to other modes.

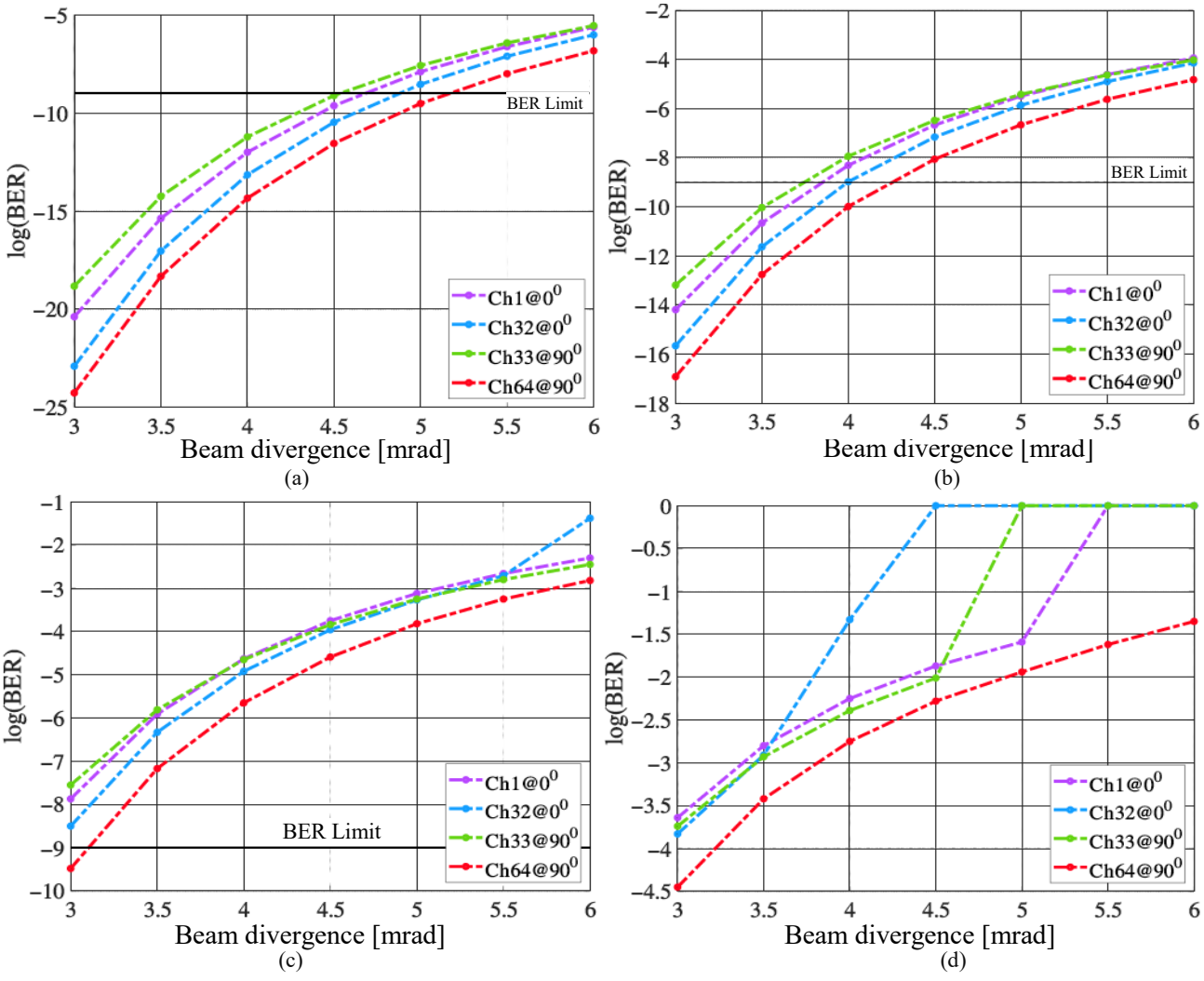

Fig. 4. Beam divergence vs. BER for (a) LG[0,0], (b) LG[1,0], (c) LG[2,0] and (d) LG[3,0] (colour online)

Fig. 4(a)-4(d) depicts the system BER performance for varied beam divergence for LG [0,0], LG[1,0], LG[2,0] and LG[3,0] modes respectively, at 0 and 90 deg angles based channels over 2000 m. It is realized that the system performs optimum for LG [0,0] than LG [1,0] which is followed by LG [2,0] and LG [3,0] modes at BER limit of 10e-9. Again, channel_64 at 90 deg performs best followed by channel_32 at 0 deg, channel_1 at 0 deg and channel_33 at 90 deg considerably. Fig. 4(a) depicts maximum beam divergence sustained by the system is 5.3, 4.8, 4.6 and 4 mrad for ch64@90, ch32@0 deg, ch1@ 0 deg and ch33@ 90 deg, respectively, for LG[0,0]. Fig. 4(b) depicts maximum beam divergence sustainability for LG[1,0] mode is 4.3, 4, 3.8 and 3.7 mrad for ch64@90,

ch32@0 deg, ch1@ 0 deg and ch33@ 90 deg, respectively. Also, for LG[2,0] mode, at BER of 10e-9, the beam divergence leads to 3.2, <3, <3 and <3 mrad for ch64@90, ch32@0 deg, ch1@ 0 deg and ch33@ 90 deg, respectively, as depicted in Fig. 4(c). Also, in Fig. 4(d), it is realized that all four channels incorporates maximum beam divergence of < 3 mrad for LG[3,0] mode. Fundamental LG [0,0] mode performs best than other modes due to the more power focused at centre compared to higher order modes. Table 3 depicts the summarized obtained results for varied beam divergence.

Table 3. Maximum acceptable beam divergence (mrad)

Channel	LG[0,0]	LG[1,0]	LG[2,0]	LG[3,0]
Channel 1 at 0 deg	4.6	3.8	<3	<3
Channel 32 at 0 deg	4.8	4	<3	<3
Channel 33 at 90 deg	4	3.7	<3	<3
Channel 64 at 90 deg	5.3	4.3	3.2	<3

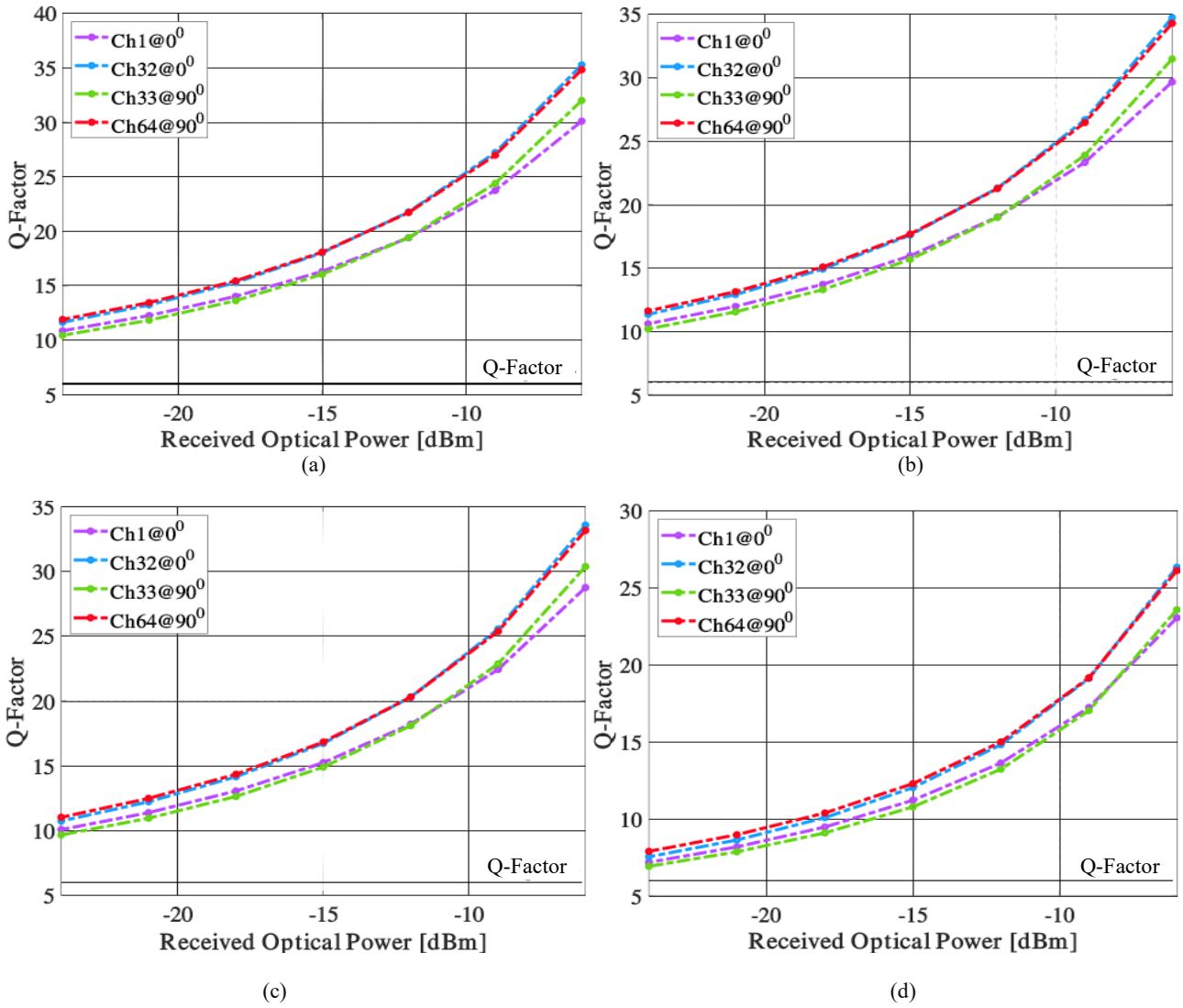

Fig. 5. Received optical power vs. Q-factor for LG[0,0] beams under (a) very clear, (b) clear, (c) light rain and (d) moderate rain conditions (colour online)

Fig. 5(a)-5(d) depicts the system performance in terms of Q factor for -24 to -6 dBm received optical power (ROP) at 2.56 Tbps data rate for LG [0,0] mode under very clear, clear, light and moderate rain conditions over 2000 m. The system performs best under very clear condition followed by clear, light and moderate rain

conditions. Fig. 5(a) depicts maximum Q factor obtained for all channels viz. Ch1@0 deg, Ch32@0 deg, Ch33@90 deg and Ch64@ 90 deg is 10.87, 11.65, 10.45 and 11.91, respectively under very clear. Also, for Ch1@0 deg, Ch32@0 deg, Ch33@90 deg and Ch64@ 90 deg channels the maximum Q factor obtained as 10.61, 11.35, 10.2 and 11.62, respectively, under clear condition, as depicted in Fig. 5(b). Again, maximum Q factor of 10.08, 10.74, 9.67 and 11.03 is achieved for Ch1@0 deg, Ch32@0 deg, Ch33@90 deg and Ch64@ 90 deg channels, respectively under light rain scenario, as depicted in Fig. 5(c). Moreover, Fig. 5(d) shows the system offers maximum Q factor of 7.19, 7.55, 6.93 and 7.9 for Ch1@0 deg, Ch32@0 deg, Ch33@90 deg and Ch64@ 90 deg channels respectively under moderate rain. Table 4 depicts the comparison analysis of the proposed work with existing works and shows superiority in terms of link capacity and transmission rate. Table 5 depicts the obtained results in terms of different factors for varied beam divergence.

Table 4. Comparative analysis w.r.t. existing works

Ref.	Data rate	Maximum range	Modulation	Channels	Weather conditions	BER
[5]	5.12 Tbps	48000 km	OFDM	8	-	10^{-3}
[2]	1.792 Tbps	1600 km	DQPSK	64	-	10^{-12}
[6]	80 Gbps	6 km	OQPSK	8	Clear air, heavy dust	10^{-6}
[7]	1600 Gbps	162 m	OOK	1	weak-to-strong	10^{-9}
This work	2.56 Tbps	4100 m	OOK	128	Very clear, clear, light and moderate rain	10^{-9}

Table 5. Obtained results

Beam divergence (mrad)	Gain (dB)	Noise Figure (dB)	Output signal (dBm)	Output OSNR(dB)
3	-28.3124	28.3124	-19.6722	80.3278
3.5	-31.651357	31.6514	-23.0111	76.9889
4	-34.057234	34.0572	-25.417	74.583
4.5	-35.939215	35.9392	-27.299	72.701
5	-37.485157	37.4852	-28.8449	71.1551
5.5	-38.797076	38.7971	-30.1568	69.8432
6	-39.936597	39.9366	-31.2963	68.7037

4. Conclusion

A 2.56 Tbps PDM/MDM-FSO system using quad LG beams viz. LG [0,0], LG[1,0], LG[2,0] and LG[3,0] modes is realized under very clear, clear, light and moderate rain conditions. The system can offers maximum FSO range of 3500-4100 m for all operating modes under very clear condition at BER of 10^{9}. It is also observed that the system can sustain beam divergence of 4-5.3 mrad for LG [0,0], 3.7-4.3 mrad for LG [1,0], 3-3.2 mrad for LG [2,0] and < 3 mrad for LG [3,0] mode under very clear condition at 2000 m range. Also, with acceptable Q-factor of 6, the received power of -24 to -6 dBm can be obtained for all operating modes under different climate conditions for fundamental mode. In future, this system can be utilized for video surveillance, cellular backhaul networks, disaster monitoring, inter-building communication, security, last mile and satellite communications.

References

[1] M. Khulbe, Harish Parthasarathy, Wirelless Communications and Mobile Computing 5355854 (2022).
[2] E. Ehsan, R. Ngah, N. A. B. Daud, Optik **269**, 169858 (2022).
[3] K. Mallick, R. Atta, N. Sarkar, B. Dutta, B. Kuiri, P. Mandal, A. S. Patra, Opt. Commun. **522**, 128699 (2022).
[4] A. Trichili, K. H. Park, M. Zghal, B. S. Ooi, M. S. Alouini, IEEE Commun. Surv. Tut. **21**, 3175 (2019).
[5] M. M. Abdulwahid, S. Kurnaz, Optik **273**, 170449 (2023).
[6] N. S. V. M. Yarra, A. Sivanantha Raja, K. Esakki Muthu, Optoelectron. Adv. Mat. **17**(9-10), 446 (2023).
[7] B. Dutta, N. Sarkar, R. Atta, B. Kuiri, A. Sekhar, Results Opt. **9**, 100287 (2022).
[8] Y. Shi, A. Armghan, F. Ali, K. Aliqab, M. Alsharari, Photonics **10**, 121 (2023).

[9] Y. Fang, J. Yu, N. Chi, J. Zhang, J. Xiao, IEEE Photonics J. **7**, 1 (2015).
[10] P. Vijayakumari, M. Sumathi, Results Phys. **14**, 102503 (2019).
[11] M. Kumari, Microw. Opt. Technol. Lett. **65**, 1822 (2024).
[12] M. Kumari, J. Opt. Commun. **56**, 546 (2024).
[13] K. Anbarasi, C. Hemanth, R. G. Sangeetha, Opt. Laser Technol. **97**, 161 (2017).
[14] R. Ullah, S. Ullah, W. A. Imtiaz, J. Khan, P. M. A. Shah, M. Kamran, J. Ren, S. Chen, Photonics **10**, 1073 (2023).
[15] M. Kumari, T. Emerg. Telecommun. T. **36**, 1 (2025).
[16] M. Kumari, R. Sharma, A. Sheetal, T. Emerg. Telecommun. T. **32**, e4214 (2021).
[17] M. Singh, S. A. Abd El-Mottaleb, H. Yousif Ahmed, M. Zeghid, K. S. Nisar, A. N. Al-Ahmadi, M. Mahmoud, Alexandria Eng. J. **77**, 15 (2023).
[18] M. Singh, A. Atieh, M. H. Aly, S. A. Abd El-Mottaleb, Alexandria Eng. J. **61**, 10407 (2022).
[19] M. Kumari, Wirel. Networks **29**, 1721 (2023).
[20] A. Niaz, F. Qamar, M. Ali, R. Farhan, M. K. Islam, T. Emerg. Telecommun. T.**30**, 1 (2019).
[21] M. Kumari, M. Banawan, V. Arya, S. K. Mishra, Photonics **10**(12), 1384 (2023).
[22] M. Kumari, V. Arya, H. M. R. Al-Khafaji, IEEE Access **11**, 43360 (2023).
[23] S. T. Mantey, M. A. Fernandes, G. M. Fernandes, N. A. Silva, F. P. Guiomar, P. Monteiro, A. N. Pinto, N. J. Muga, J. Light. Technol. **43**, 1043 (2025).

*Corresponding author: ichvivekmalik@gmail.com